



## Effect of Surface Chemical Modification on the Self Assembly of Metal Nanoparticles

Mona Samir<sup>a,c</sup>, Dina Salah<sup>b\*</sup>, Shafei Donia<sup>c</sup>, Amal Kasry<sup>a\*</sup>

<sup>a</sup> Nanotechnology Research Center (NTRC), the British University in Egypt (BUE),

El-Shorouk City, Suez Desert Road, Cairo 11837 - P.O. Box 43, Egypt.

<sup>b</sup> Physics department, Faculty of Science, Ain Shams University, Khalifa El-Maamon Street, 11566, Cairo, Egypt.

<sup>c</sup> Chemistry Department, Faculty of Science, Benha University, Benha 13518, Egypt.



CrossMark

**Abstract.** We report the self-assembly of monolayer of gold nanoparticles (Au-NPs) on unmodified glass and on functionalized glass substrates with 3-aminopropyltriethoxysilane under different temperatures. The interaction between Au-NPs and APTES molecules on the glass substrates was affected by the role of APTES molecules on the glass substrates. The stability of the monolayers was carefully studied by performing a series of characterizations such as UV-Vis-NIR spectroscopy, Scanning electron microscopy (SEM). The self-assembled Au-NPs monolayers show high stability and homogenous distribution. The results of this study are important biosensing applications based on surface plasmon resonance or surface-enhanced Raman spectroscopy, where the detected signals can be adequately enhanced.

*Keywords:* Self-assembly; Gold-Nanoparticles; Surface plasmon resonance (SPR).

### 1. Introduction

In the past few decades, metals in the nanoscale dimensions have attracted a great attention and were of great potential in several chemical [1], photonic [2], electronic [3], and biological applications [4-6]. Therefore, self-assembled gold nanoparticles (Au-NPs) showed a great scientific and technological interest.

Metallic Nanoparticles (NPs) could vary in size and shape [7,8], and their self assembly[9-12] was studied due to their great potential. When self-assembled, their initial bulk concentrations affect their final distribution on the surface. Using cross-linking agents, such as; thiol-based molecules, was found to affect both the surface the NPs bonding strength to the surface, it also increases its stability [13,14]. Chemically-modified surfaces with APTES (source of NH<sub>2</sub>-terminal molecule) were widely used in various applications that includes Surface plasmon resonance (SPR) [15-17].

Due to the quantum confinement, high surface areas, and their ability to be functionalized with various compounds that can increase their stability and their equal distribution on the surface, NPs can be used in several applications, e.g. chemical and biological sensing[18,19], drug delivery[20], may biomedical applications[21] as cancer nanotechnology[22], virus detection[23].

Various techniques were used to deposit gold layers on different surfaces. In our experiments we relied on glass substrates. Those techniques were developed to achieve stable Au NPs layers, homogeneous surfaces, high surface morphology, and self-organization. Moreover, those techniques are easy, flexible, and inexpensive. Deposition of gold nanoparticles has been reported on different surfaces using spray pyrolysis with temperature ranging between 75-320°C [24] and also by spin coating [25].

Indeed, concentration variations, NPs method of preparation, and the deposition techniques on the surface are among the factors affecting the formation of the layer. In the present study, Au-NPs were

\*Corresponding authors e-mail: [Amal.Kasry@bue.edu.eg](mailto:Amal.Kasry@bue.edu.eg), [dinasalah@sci.asu.edu.eg](mailto:dinasalah@sci.asu.edu.eg)

Receive Date: 12 July 2021, Revise Date: 25 July 2021, Accept Date: 26 July 2021

DOI: [10.21608/EJCHEM.2021.85558.4160](https://doi.org/10.21608/EJCHEM.2021.85558.4160)

©2022 National Information and Documentation Center (NIDOC)

prepared by using CTAB as stabilizing agent and sodium borohydride as a reducing agent. The resultant gold nanoparticle solution is 5 nM concentration, then sodium thioglycolate was added with optimum concentration as a source of thiol groups to prevent gold particles aggregation and allow preservation for longer time in the desired size. The  $\text{NH}_2$  groups were formed on the glass surface by dipping the pre-cleaned glass in a pre-prepared APTES solution [26]. Afterwards, glass samples were dipped in the used solvent for the removal of the unattached functional groups/ molecules. Then, drop-casting technique was employed to assemble Au-NPs.

A comparison was made between the Au-NPs layers on both APTES-modified and unmodified glass substrates.

In parallel to that, the above-mentioned procedures were applied but with an extra step, which is annealing at a temperature  $300^\circ\text{C}$  in order to study the effect of the annealing on the self-assemble layers.

## 2. Experimental:

**Gold nanoparticles preparation:** a solution with a concentration of 5nM was prepared with average size between 25 nm and 30 nm and optimum absorption of 527 nm according to the Turkevich-Frens [27,28], and as previously reported [29]. Functionalization was achieved by dissolving sodium Thioglycolate

separately in water with a concentration of 0.05 mM, then it was added to gold (5nm) to prepare thiolated gold nanoparticles with concentration of 0.5 nm.

**Au-NPs monolayer preparation:** on the functionalized and unfunctionalized glass samples were cleaned by sonication in ethanol for 15 mins. Glass samples were activated by dipping in a solution of APTES with concentration of 1mg/ml for 3 hrs. Samples were then washed and dried. Thiolated gold solution was dropped using the drop-casting technique, directly on the activated/functionalized glass and then it was dried in the air. The unfunctionalized glass substrate was washed with ethanol, dried in the air, and then gold was dropped afterwards.

**The annealing process:** Both functionalized and unfunctionalized surfaces were heated up to  $300^\circ\text{C}$ . After gold deposition on APTES activated/modified surface, the sample were annealed at  $300^\circ\text{C}$ . regarding the untreated samples, gold was deposited on glass and heated at  $300^\circ\text{C}$ .

**Characterization:** surface imaging was performed using Field emission scanning electron microscope (FESEM) (Thermo Scientific, FESEM Quattro S, USA). Absorption spectra was measured by Uv-Vis-NIR spectrophotometer (Agilent Cary5000, USA).

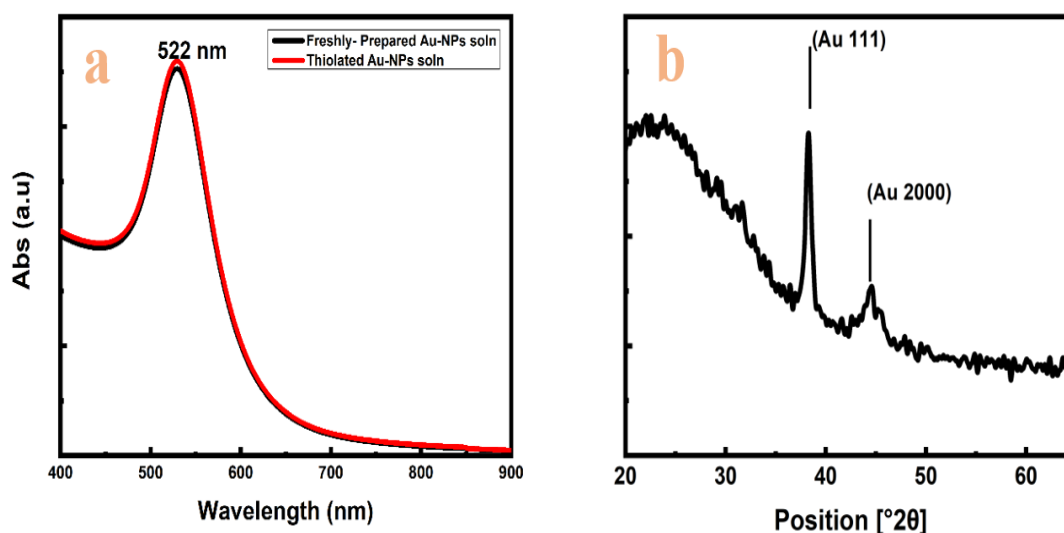


**Figure 1.** (a) UV-visible absorption spectra of Au-NPs solution with a characteristic absorption  $\lambda_{\text{max}} = 522$  nm. (b) XRD patterns for Au-NPs deposited onto glass substrate at room temperature

### 3. Results and Discussion

#### 3.1 Optical and Structural properties for bulk solution

Figure 1a shows the UV-Vis absorption spectra of AuNPs as-prepared solution, and after the thiolation process by sodium thioglycolate. It shows that there is no change in the absorption peak. The XRD pattern of Au-NPs assembled on glass (Figure 1b) reveal peaks at 2 different theta values 38.2 and 44.3 degrees which represent the reflection from (111) and (200) planes of metallic Au indicating a cubic structure. The metallic Au peak (Au 111) was used to calculate the mean crystallite size of A-NPs by the Scherrer formula [30]. The mean value of the XRD patterns correspond to a crystallite size of Au-NPs between 25 and 40 nm. For the annealed samples, the crystalline size decrease and Au-NPs show low intensity with a broad peak.

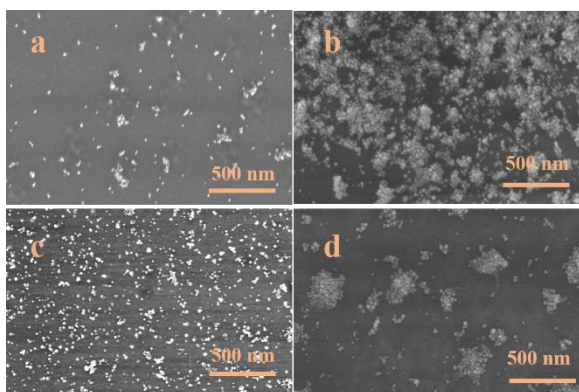


**Figure 2.** SEM images of the drop casted Au-NPs deposited onto glass substrates at various deposition temperatures: (A) without APTES; RT. (B) with APTES; RT. (C) without APTES; 300 °C. (D) with APTES, 300 °C.

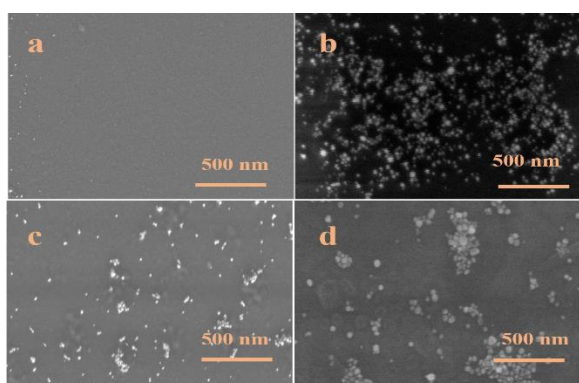


**Figure 3.** SEM images (after 1 hr water sonication) of the drop casted Au-NPs deposited onto glass substrates: (A) without APTES; RT. (B) with APTES; RT. (C) without APTES, 300 °C. (D) with APTES; 300 °C.

#### 3.2 Element morphology and composition

The fresh-prepared solution of Au NPs has a pink color, which indicates particles' size of not more than 30 nm. The SEM images showed a clear difference in the distribution of the Au NPs on the unmodified and modified glass surfaces.

Figure 2 shows the morphology of the surface for each of the samples that were prepared at room temperature and at a temperature of 300°C, with and without APTES. Figure 2A shows the Au-NPs deposited on unmodified glass at room temperature, where it is clear that the surface is not homogenous. Figure 2B shows the NPs deposited on APTES-modified glass. Figure 2 C and D show the deposited NPs on unmodified and modified glass, respectively, and annealed at 300°C, it is obvious that the APTES causes the NPs to aggregate and form inhomogenous surface, while on the unmodified glass, the NPs form nicely homogenous layer.

Au-NPs layer stability has been studied by sonicating the substrates at high power for one hour. As Figure 3 shows, the annealing had a big effect on the homogeneity and stability of the layers, where washing and sonicating of the layer deposited on unmodified glass led to almost full removal, while washing the layer on the APTES-modified glass didn't affect the layer. On the other hand, washing the annealed layer on the unmodified glass reveals a level of stability, while the annealed layer on modified glass was similar to the one without annealing, where high level of aggregation was observed.

#### 3.3 Optical properties for Au-NPs layer

The stability of the deposited layers was examined by measuring the optical absorption on the surface. since metallic nanoparticles exhibit absorption in the visible because of their surface plasmons properties, monitoring optical absorption becomes an easy and quick tool to study the NPs size and density. Figure 4a shows the optical absorption of the Au-NPs layer deposited at room temperature on the unmodified glass substrate, before and after sonication, which clearly shows the instability of the layer in this case, where there is no absorption, indicating that it was completely removed.

This is while the same layer deposited on APTES-modified glass at room temperature shows very good stability, where the absorption peak remains visible after several sonicating steps, with no major changes in the wavelength. When repeating the same, but combined with annealing at 300°C, the layers show great stability (Figure 4 c and d), however in case of

the layer deposited on APTES-modified surface, a clear shift in the absorption is observed, which is due to the aggregation of the NPs, as was clearly seen by the SEM imaging (Figure 2d and 3d).

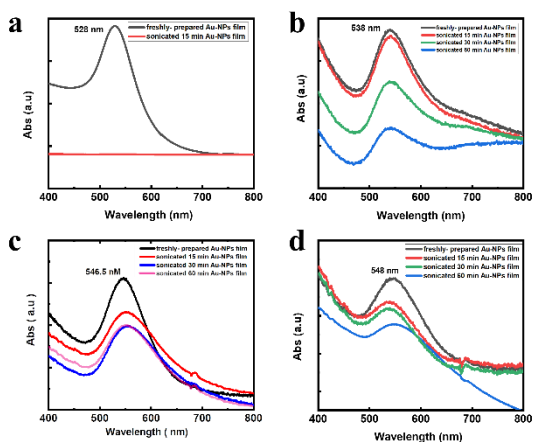


**Figure 4. Stability Test of self-assembled Au-NPs on glass substrates.** UV-visible absorption spectra of AuNPs assembled on glass substrate before and after sonication for different times; 15 min, 30 min, and 60 min. (a) Au-NPs layer deposited on glass, (b) Au-NPs deposited on APTES-functionalized glass, (c) Au-NPs deposited on glass at 300 °C, and (d) for Au-NPs deposited on APTES-functionalized glass with 300 °C.

#### 4. Conclusions

In this work, we investigated the possibility to self-assemble Au-NPs on glass surface using easy and inexpensive method. We have used drop-casting method where the NPs were deposited on unmodified and APTES-modified glass substrates, with applying another condition, which is annealing the deposited layers at 300 °C, and comparing the results with the unannealed samples.

The results clearly indicate that we can control the density of the NPs on the surface by combining these two factors; the chemical modification and the temperature. The deposited layer on unmodified layer showed good stability with much less NPs density than that deposited on APTES-modified surface. The level of aggregation was also shown to be dependent on the both the chemical modification and temperature, where combining both led the NPs to aggregate to a great extent.

The stability of the layers were tested with both SEM imaging and absorption spectra, where the optical absorption was measured after different sonication time, and the aggregation was translated to a shift in the absorption wavelength.

This work introduces an easy, inexpensive, and reproducible method to self-assemble monolayers of

metallic nanoparticles on glass surfaces, which is important for several applications, e.g. biosensing.

#### 5. Conflicts of interest

The authors declare no conflict of interest.

#### 6. Acknowledgments

This work was performed at the Nanotechnology research center (NTRC) at the British University in Egypt.

#### 7. References

- [1] Ibañez, F. J.; Zamborini, F. P. Chemiresistive Sensing with Chemically Modified Metal and Alloy Nanoparticles. *Small* **2012**, *8* (2), 174–202. <https://doi.org/10.1002/sml.201002232>.
- [2] Filatov, D. O.; Gorshkov, O. N.; Antonov, D. A.; Shenina, M. E.; Sinutkin, D. Y.; Zenkevich, A. V.; Matveev, Y. A. The Generation of the Electrical Oscillations in a Contact of an AFM Probe to an Individual Au Nanoparticle in a SiO<sub>2</sub>/Si Film. *IOP Conf. Ser. Mater. Sci. Eng.* **2017**, *256* (1), 0–5. <https://doi.org/10.1088/1757-899X/256/1/012006>.
- [3] Dogan, E.; Ozkazanc, E.; Ozkazanc, H. Multifunctional Polyindole/Nanometal-Oxide Composites: Optoelectronic and Charge Transport Properties. *Synth. Met.* **2019**, *256* (July), 116154. <https://doi.org/10.1016/j.synthmet.2019.116154>.
- [4] Kneipp, K.; Kneipp, H.; Kneipp, J. Surface-Enhanced Raman Scattering in Local Optical Fields of Silver and Gold Nanoaggregates - From Single-Molecule Raman Spectroscopy to Ultrasensitive Probing in Live Cells. *Acc. Chem. Res.* **2006**, *39* (7), 443–450. <https://doi.org/10.1021/ar050107x>.
- [5] Bedford, E. E.; Spadavecchia, J.; Pradier, C. M.; Gu, F. X. Surface Plasmon Resonance Biosensors Incorporating Gold Nanoparticles. *Macromol. Biosci.* **2012**, *12* (6), 724–739. <https://doi.org/10.1002/mabi.201100435>.
- [6] Yoshito Tanaka, Hiroyasu Ishiguro, Hideki Fujiwara, Yukie Yokota, Kosei Ueno, Hiroaki Misawa, and Keiji Sasaki, "Direct imaging of nanogap-mode plasmon-resonant fields," *Opt. Express* **19**, 7726–7733 (2011) <https://doi.org/10.1364/OE.19.007726>
- [7] Abdelrahman, A. I.; Mohammad, A. M.; El-Deab, M. S.; Okajima, T.; Ohsaka, T. Bisthiol-Assisted Multilayers' Self-Assembly of Gold Nanoparticles: Synthesis, Characterization, Size Control and Electrocatalytic Applications. *Macromol. Symp.* **2008**, *270* (1), 74–81. <https://doi.org/10.1002/masy.200851009>.
- [8] Sardar, R.; Funston, A. M.; Mulvaney, P.; Murray, R. W. Gold Nanoparticles: Past, Present,

- and Future. *Langmuir* **2009**, *25* (24), 1384–13851. <https://doi.org/10.1021/la9019475>.
- [9] Abdelrahman, A. I.; Mohammad, A. M.; Okajima, T.; Ohsaka, T. Fabrication and Electrochemical Application of Three-Dimensional Gold Nanoparticles: Self-Assembly. *J. Phys. Chem. B* **2006**, *110* (6), 2798–2803. <https://doi.org/10.1021/jp056238x>.
- [10] Lau, C. Y.; Duan, H.; Wang, F.; He, C. Bin; Low, H. Y.; Yang, J. K. W. Enhanced Ordering in Gold Nanoparticles Self-Assembly through Excess Free Ligands. *Langmuir* **2011**, *27* (7), 3355–3360. <https://doi.org/10.1021/la104786z>.
- [11] Okamoto, T.; Yamaguchi, I. Optical Absorption Study of the Surface Plasmon Resonance in Gold Nanoparticles Immobilized onto a Gold Substrate by Self-Assembly Technique. *J. Phys. Chem. B* **2003**, *107* (38), 10321–10324. <https://doi.org/10.1021/jp034537l>.
- [12] Liu, Y.; Lin, X. M.; Sun, Y.; Rajh, T. In Situ Visualization of Self-Assembly of Charged Gold Nanoparticles. *J. Am. Chem. Soc.* **2013**, *135* (10), 3764–3767. <https://doi.org/10.1021/ja312620e>.
- [13] Stetsenko, M. O.; Rudenko, S. P.; Maksimenko, L. S.; Serdega, B. K.; Pluchery, O.; Snegir, S. V. Optical Properties of Gold Nanoparticle Assemblies on a Glass Surface. *Nanoscale Res. Lett.* **2017**, *12*. <https://doi.org/10.1186/s11671-017-2107-8>.
- [14] Sardar, R.; Funston, A. M.; Mulvaney, P.; Murray, R. W. Gold Nanoparticles: Past, Present, and Future. *Langmuir* **2009**, *25* (24), 13840–13851. <https://doi.org/10.1021/la9019475>.
- [15] Kim, S.; Lee, J.; Lee, S. J.; Lee, H. J. Ultra-Sensitive Detection of IgE Using Biofunctionalized Nanoparticle-Enhanced SPR. *Talanta* **2010**, *81* (4–5), 1755–1759. <https://doi.org/10.1016/j.talanta.2010.03.036>.
- [16] Springer, T.; Ermini, M. L.; Špačková, B.; Jabloňková, J.; Homola, J. Enhancing Sensitivity of Surface Plasmon Resonance Biosensors by Functionalized Gold Nanoparticles: Size Matters. *Anal. Chem.* **2014**, *86* (20), 10350–10356. <https://doi.org/10.1021/ac502637u>.
- [17] Bedford, E. E.; Spadavecchia, J.; Pradier, C.; Gu, F. X. Surface Plasmon Resonance Biosensors Incorporating Gold Nanoparticles. **2012**, 1–16. <https://doi.org/10.1002/mabi.201100435>.
- [18] Saha, K.; Agasti, S. S.; Kim, C.; Li, X.; Rotello, V. M. Gold Nanoparticles in Chemical and Biological Sensing. *Chem. Rev.* **2012**, *112* (5), 2739–2779. <https://doi.org/10.1021/cr2001178>.
- [19] Dreaden, E. C.; Alkilany, A. M.; Huang, X.; Murphy, C. J.; El-Sayed, M. A. The Golden Age: Gold Nanoparticles for Biomedicine. *Chem. Soc. Rev.* **2012**, *41* (7), 2740–2779. <https://doi.org/10.1039/c1cs15237h>.
- [20] Ghosh, P.; Han, G.; De, M.; Kim, C. K.; Rotello, V. M. Gold Nanoparticles in Delivery Applications. *Adv. Drug Deliv. Rev.* **2008**, *60* (11), 1307–1315. <https://doi.org/10.1016/j>.
- [21] addr.2008.03.016. Shah, M.; Badwaik, V. D.; Dakshinamurthy, R. Biological Applications of Gold Nanoparticles. **2014**. <https://doi.org/10.1166/jnn.2014.8900>.
- [22] Huang, X.; El-sayed, M. A. Gold Nanoparticles : Optical Properties and Implementations in Cancer Diagnosis and Photothermal Therapy. **2010**, 13–28. <https://doi.org/10.1016/j>.
- [23] jare.2010.02.002. Draz, M. S.; Shafiee, H. The Applications of Gold Nanoparticles in Virus Detection. **2018**, *8* (7). <https://doi.org/10.7150/thno.23856>.
- [24] Acik, I. O.; Oyekoya, N. G.; Mere, A.; Katerski, A.; Mikli, V.; Krunks, M. In-Situ Deposition of Gold Nanoparticles onto Different Substrates by Chemical Spray Pyrolysis. *IOP Conf. Ser. Mater. Sci. Eng.* **2015**, *77* (1). <https://doi.org/10.1088/1757-899X/77/1/012009>.
- [25] Farid, S.; Kuljic, R.; Poduri, S.; Dutta, M.; Darling, S. B. Tailoring Uniform Gold Nanoparticle Arrays and Nanoporous Films for Next-Generation Optoelectronic Devices. *Superlattices Microstruct.* **2018**, *118*, 1–6. <https://doi.org/10.1016/j.spmi.2018.04.006>.
- [26] Xu, X.; Stevens, M.; Cortie, M. B. In Situ Precipitation of Gold Nanoparticles onto Glass for Potential Architectural Applications. *Chem. Mater.* **2004**, *16* (11), 2259–2266. <https://doi.org/10.1021/cm034744y>.
- [27] Daniel, M. C.; Astruc, D. Gold Nanoparticles: Assembly, Supramolecular Chemistry, Quantum-Size-Related Properties, and Applications Toward Biology, Catalysis, and Nanotechnology. *Chem. Rev.* **2004**, *104* (1), 293–346. <https://doi.org/10.1021/cr030698+>.
- [28] Stetsenko, M. O.; Rudenko, S. P.; Maksimenko, L. S.; Serdega, B. K.; Pluchery, O.; Snegir, S. V. Optical Properties of Gold Nanoparticle Assemblies on a Glass Surface. *Nanoscale Res. Lett.* **2017**, *12*. <https://doi.org/10.1186/s11671-017-2107-8>.
- [29] Chadwick, S. J.; Salah, D.; Livesey, P. M.; Brust, M.; Volk, M. Singlet Oxygen Generation by Laser Irradiation of Gold Nanoparticles. *J. Phys. Chem. C* **2016**, *120* (19), 10647–10657. <https://doi.org/10.1021/acs.jpcc.6b02005>.
- [30] Icimoto, M. Y.; Brito, A. M. M.; Ramos, M. P. C.; Oliveira, V.; Nantes-Cardoso, I. L. Increased Stability of Oligopeptidases Immobilized on Gold Nanoparticles. *Catalysts* **2020**, *10* (1). <https://doi.org/10.3390/catal10010078>.